Conf-9310261--5

PNL-SA-23096

SCINTILLATING GLASS FIBER NEUTRON SENSORS: II. LIGHT TRANSMISSION IN SCINTILLATING FIBERS

M. Bliss

October 1993

Presented at the
Workshop on Scintillating Fiber Detectors
October 24-28, 1993
South Bend, Indiana

Work supported by
the U.S. Department of Energy
under Contract DE-AC06-76RLO 1830

MASTER

DISTRIBUTION OF THIS DOCUMENT IS UNLIMITED

Pacific Northwest Laboratory
Richland, Washington 99352

DISCLAIMER

SCINTILLATING GLASS FIBER NEUTRON SENSORS: II. LIGHT TRANSMISSION IN SCINTILLATING FIBERS

K. H. Abel, R. J. Arthur, M. Bliss, D. W. Brite, R. L. Brodzinski, R. A. Craig, B. D. Geelhood, D. S. Goldman, J. W. Griffin, R. W. Perkins, P. L. Reeder, W. C. Richey, K. A. Stahl, D. S. Sunberg, R. A. Warner, and N. A. Wogman
Pacific Northwest Laboratory, Box 999, Richland, WA 99352

and

M. J. Weber
Lawrence Livermore Laboratory, Box 808, Livermore, CA 94551

ABSTRACT

The capture and transmission of light from an event through a scintillating fiber is somewhat different than in conventional optical waveguide applications. A theoretical all–ray model that depends on surface and bulk loss factors is developed for this transmission. The capture fraction can be significantly greater than that predicted on the basis of meridional rays alone and the gross loss is nonexponential for short distances (less than or of the order of one 1/e distance). The latter phenomenon occurs because high-angle and skew rays are more rapidly attenuated than meridional rays.

1. Introduction

The propagation of light in scintillating fibers differs from that for common optical waveguides because of the dissimilarity of the launching conditions. Common optical waveguides are designed and characterized under the assumption that parallel light rays are injected into the waveguide at one end. In the case of scintillating or fluorescing fibers the light is generated internally and radiates in all directions. Only a small fraction of the light generated can be captured by the waveguide. The purpose of this study is to develop a theory of capture and transport of light for scintillating fibers.

In addition to providing insight into the details of the capture and transmission of photons, this study explains the experimental observation that light extinction in the fibers is not logarithmic.[a] This work will address launching and propagation of all rays instead of just meridional rays (those which pass through the axis of the fiber).

The specific model used here for the scintillating fiber includes the following assumptions:

- The fiber is a circular cylinder.
- Cladding rays (i.e., rays propagating in the cladding) are unimportant.
- The fiber diameter is sufficiently large that ray optics can be used.

[a] See, for instance, reference 1.

- There are two components to loss in the fiber: bulk extinction and loss on reflection.
- Monochromatic light is addressed.[b]

2. Theory

This calculation assesses the capture and propagation of photons emitted from a general position within the core. Photons emitted by activators on the axis of the fiber are meridional and the standard calculations apply to these. Photons emitted by activators off the axis mostly are categorized as skew and follow a more complicated set of rules than for the meridional case. We will address the propagation and capture of internally generated photons using a ray approach. This work is perfectly general and includes meridional photons as a special case.

Propagation will be addressed first because it helps to introduce the appropriate geometry. In understanding skew rays, the proper choice of geometry can be a significant help.[2] Consider Figure 1. This cylinder represents the core of the fiber; the surface of the cylinder is the core/cladding interface. The refractive index of the core is n_1, that of the cladding n_2. The radius of the fiber is a. Figure 2 shows the projection of Figure 1 onto a plane perpendicular to the axis of the cylinder (plane KBC). The plane of propagation, KK'B'B, contains the ray segment propagating down the fiber and is parallel to the axis of the fiber. The angle ψ is the angle between the ray and the radius, CK; that is, ψ is the angle of incidence with the core/cladding interface. The angle θ is the angle between the ray segment and a line parallel to the axis of the cylinder lying in the plane of propagation. The angle γ is the angle between the radius, CK, and the intersection of the plane KK'B'B with the normal to the cylinder. Point S is a point on the line KB (the line defined by the intersection of KK'B'B and KBC). The point T is the intersection with the radius CK of a line drawn perpendicular to CK from S in the plane KBC. TM is a line perpendicular to CK such that the angle TKM is the angle of incidence, ψ.

Following the analysis of Drougard and Potter[2],

$$\cos(\psi) = KT/KM.$$

Now

$$\sin(\theta) = KS/KM \quad \text{and} \quad \cos(\gamma) = KT/KS.$$

So that

$$\cos(\psi) = \cos(\gamma)\,\sin(\theta) \qquad (1)$$

---

[b] The extension to polychromatic radiation will be discussed.

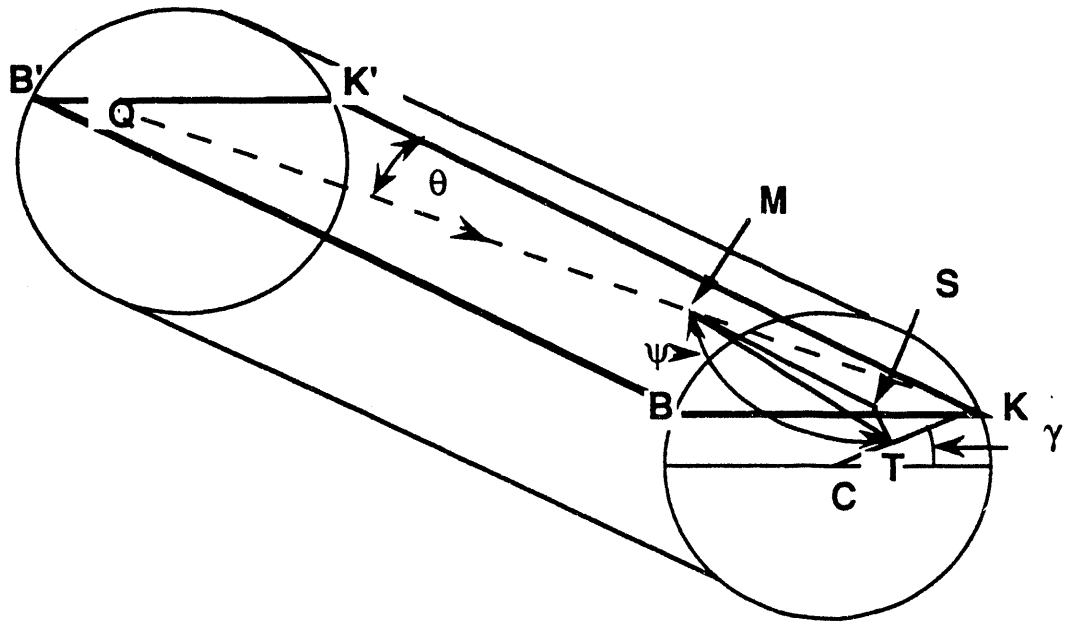

Figure 1. Geometry used for analysis of skew rays. The skew ray is the dotted line QK. C is the axis of the fiber core.

Since the condition for total internal reflection is $\sin(\psi) \geq n_2/n_1$, Eq.(1) translates into

$$\cos(\gamma)\,\sin(\theta) \leq \sqrt{1-(n_2/n_1)^2}. \qquad (2)$$

This is an important result. By Snell's law, ψ is preserved at each reflection and, since (γ) is preserved at each reflection (this is the projection of equal angles onto a plane), then (θ) is also preserved at each reflection. (The ray-containing plane projects onto the plane perpendicular to the cylinder axis as shown in Figure 2.) From Figure 1 it is easy to see that the distance a ray travels in the core medium, per unit distance traveled down the length of the fiber, is simply $1/\cos(\theta)$. Thus, in the model described above, the light loss due to intrinsic extinction[c] is

$$\left.\frac{dI}{dz}\right|_{abs} = -\alpha\, I(z)/\cos(\theta) \qquad (3a)$$

in which α is the extinction coefficient and I(z) is the intensity at a point z.

The distance travelled along the axis of the cylinder between reflections, L, is, from Figures 1 and 2

[c] Extinction refers to intrinsic absorption, bulk scattering, or bulk fluorescence (the last of which manifests itself as bulk scattering).

$$L = 2a\cos(\gamma)/\tan(\theta).$$

If we designate the loss at each reflection[d] to be Δ, then the differential loss due to loss-on-reflection mechanisms is

$$\frac{dI}{dz_{lref}} = -\Delta I(z)/L = -[\Delta \tan(\theta)/2a\cos(\gamma)]I(z) \qquad (3b)$$

We can combine Eqs.(3a) and (3b) into a single propagation equation. However, first it

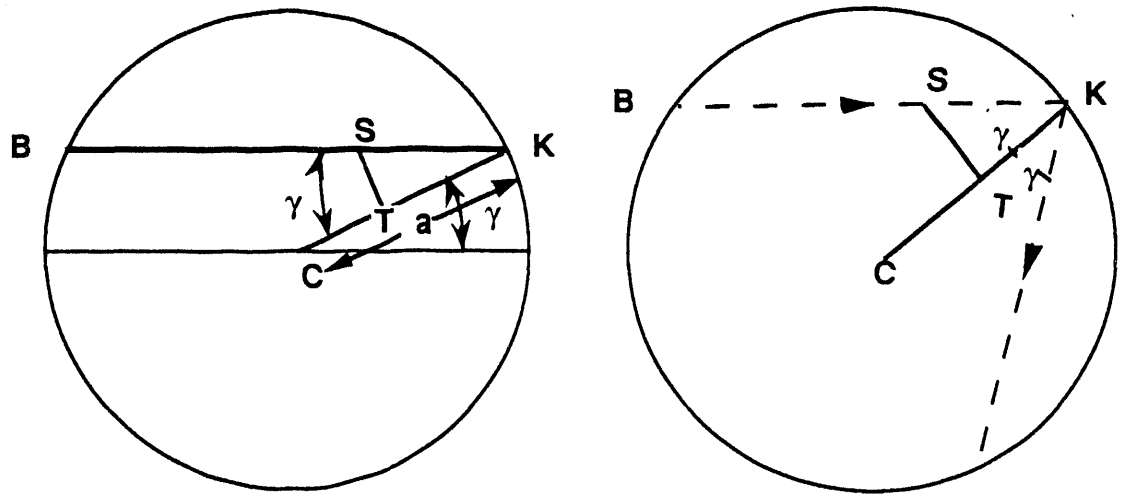

Figure 2. Left figure is an end view of fiber and shows the geometry defined in Figure 1. C is the axis of the fiber core. Right view shows projection of a the path, including the path after the first reflection, of a skew ray locus (dotted line) onto the plane perpendicular to fiber.

is appropriate to address the capture fraction of rays, including those that may originate off the axis. Consider Figure 3, which shows a projection onto a plane perpendicular to the axis of the cylinder of the locus of an off-axis-generated ray. The ray originates from the point O; the projection onto this plane of the ray locus makes an angle ϕ with a radius through O. Now, by the law of sines,

$$[\sin(\gamma)]/r = [\sin(\pi - \phi)]/a = [\sin(\phi)]/a.$$

Therefore,

$$\sin(\gamma) = (r/a)[\sin(\phi)].$$

---

[d] Without specifying the cause of this loss.

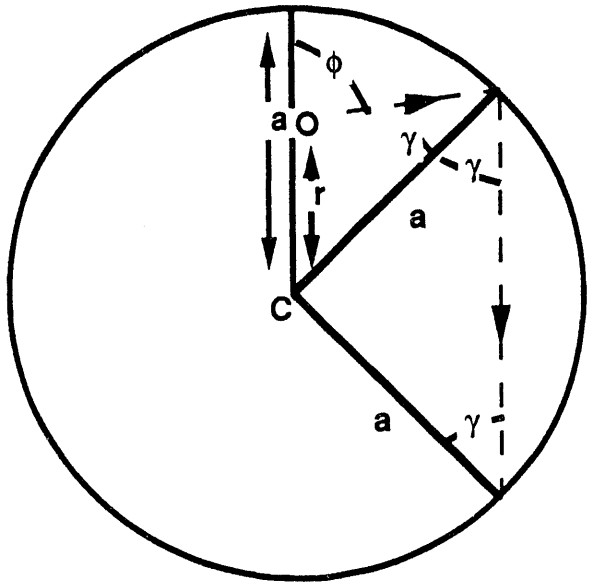

Figure 3. Projection of a ray locus (dotted line) onto the plane perpendicular to fiber axis for a skew ray emitted at point O. Point O is a distance r from the center of the fiber; the ray being considered makes an angle ϕ with the radius. The fiber radius is a. Other parameters are as defined earlier. Not seen in this perspective, the ray also makes an angle θ with a line parallel to the axis of the core.

Thus, the propagation of a ray originating at O, a distance r from the axis of the core, with angles θ and ϕ, as shown in Figures 1 and 3, is governed by the differential equation

$$\frac{dI}{dz} = -\{[\alpha/\cos(\theta)] + [\Delta \tan(\theta)/2a \cos(\gamma)]\}I$$

with solution

$$I(z;r,\theta,\phi) = I_0 e^{-([\alpha/\cos(\theta)] + [\Delta \tan(\theta)/2a\cos(\gamma)])z} \qquad (4)$$

where

$$\cos(\gamma) = \sqrt{1-(r/a)^2\sin^2(\phi)} \qquad (5)$$

and

I_0 = the intensity at the point of emission.

Note that the dependence of $I(z;r,\theta,\phi)$ on the radial position of the emitting activator enters through Eq.(5).To calculate the fraction of the emitted light which is retained within the system as a function of distance, we

1) perform an unrestricted integration of Eq.(4) over the plane at z=0 and over all angles of photon emission, θ and ϕ, with the point of observation at z=0.

2) perform the same integration of Eq.(4) subject to the condition of total internal reflection with the point of observation at z.

The ratio of these two integrals, I_2/I_1, yields the fraction, f(z), of the emitted light still retained as a function of distance. The first integral, I_1, is

$$I_1 = 2\pi I_0 \int_0^a r\,dr \int_0^{\pi} \sin(\theta)\,d\theta \int_0^{2\pi} d\phi$$

$$= 4\,\pi^2\,a^2\,I_0.$$

The second integral is

$$I_2 = 2\pi I_0 \int_0^a r\,dr \int_0^{\pi/2} \sin(\theta)\,d\theta \int_0^{2\pi} d\phi \cdot e^{-([\alpha/\cos(\theta)] + [\Delta \tan(\theta)/2a\cos(\gamma)])z}$$

subject to the condition

$$\cos(\gamma)\sin(\theta) \le \sqrt{1-(n_2/n_1)^2}.$$

Noting that γ is symmetric in ϕ about $\pi/2$, converting to dimensionless variables via

$$u = (r/a)^2 \qquad x = \cos(\theta) \quad \text{and} \quad \phi = \pi v/2,$$

and performing the division of integrals, the light fraction remaining at any distance is

$$f(z) = 1/2 \int_0^1 du \int_0^1 dx \int_0^1 dv \cdot \exp -\{(z/x)(\alpha + [\Delta \sqrt{(1-x^2)}/2a \sqrt{(1 - u \sin^2(\pi v/2))}])\} \qquad (6)$$

subject to the total reflection condition

$$\sqrt{(1-x^2)}\,\sqrt{(1 - u \sin^2((\pi/2)v))} \le \sqrt{1-(n_2/n_1)^2}.$$

The integral in Eq.(6) does not appear to be amenable to closed form integration so it has been evaluated numerically.

We examined the relative effect of reflection loss versus extinction loss. In order to compute the relative effect of these two loss mechanisms, the locus of values of α and δ ($= \Delta/2a$) for which the captured light is reduced to one-half the original value when $z = 1$ was calculated. This establishes a length scale. Then the fractional remaining intensity was calculated for these pairs of α and δ as a function of z. The distance, z, is measured in units of the initial half-length; that is at $z = 1.0$, the fraction of light remaining is one-half the initial value. The results for four such pairs of α and δ in Figure 4 clearly show that there is a significant difference in the shape of the loss curve as a function of distance for the different loss mechanisms. If the loss is predominantly via bulk extinction, the effective loss coefficient is nearly constant with distance; if the loss is predominantly due to reflection, the effective loss coefficient will be constantly decreasing with length. Consequently, it may be possible to distinguish between the two loss mechanisms by experiment.

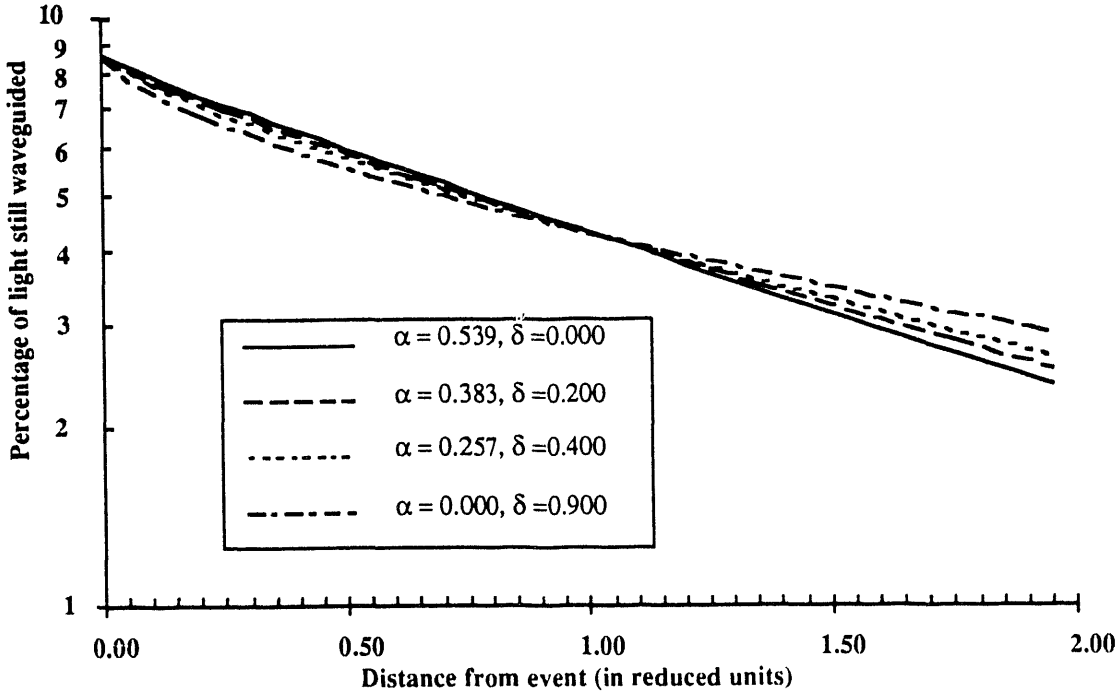

Figure 4. Fraction of total emitted light remaining vs. reduced distance for various values of α and δ. Here $\delta = \Delta/2a$ is the loss-on-reflection coefficient.

3. Conclusions

The results of this study lead to two rather simple conclusions. First, meridional calculations are conservative. That is, such calculations significantly underpredict the captured fraction of the photons produced by the scintillation event. The reason for this underprediction is that scintillation events occurring off-axis produce skew rays which, because they spiral down the fiber, have a path length substantially longer than that

predicted by meridional calculations. Not only do they travel a greater distance through the core, they also have more interactions with the core/cladding interface per unit distance travelled down the fiber. As a result, the distribution of rays remaining becomes increasingly directed along the axis the further down the fiber. This appears as an effective decrease in numerical aperture the further the event is from the fiber end.

Second, the differing extinction rate per unit distance down the fiber of different classes of rays (that is, in this case, rays with different angles with respect to the fiber axis) results in a non-exponential decay for the collective (that is, all rays) extinction. The exact shape of the non-exponential extinction depends on the loss mechanisms in the fiber. This also provides insight into what happens when there is a mix of rays with different extinction coefficients for other causes, such as when there is dispersion in the extinction. In this case, also, the result will be a non-exponential loss curve for each angle. If the two situations are combined the result will be a more complicated non-exponential loss curve.

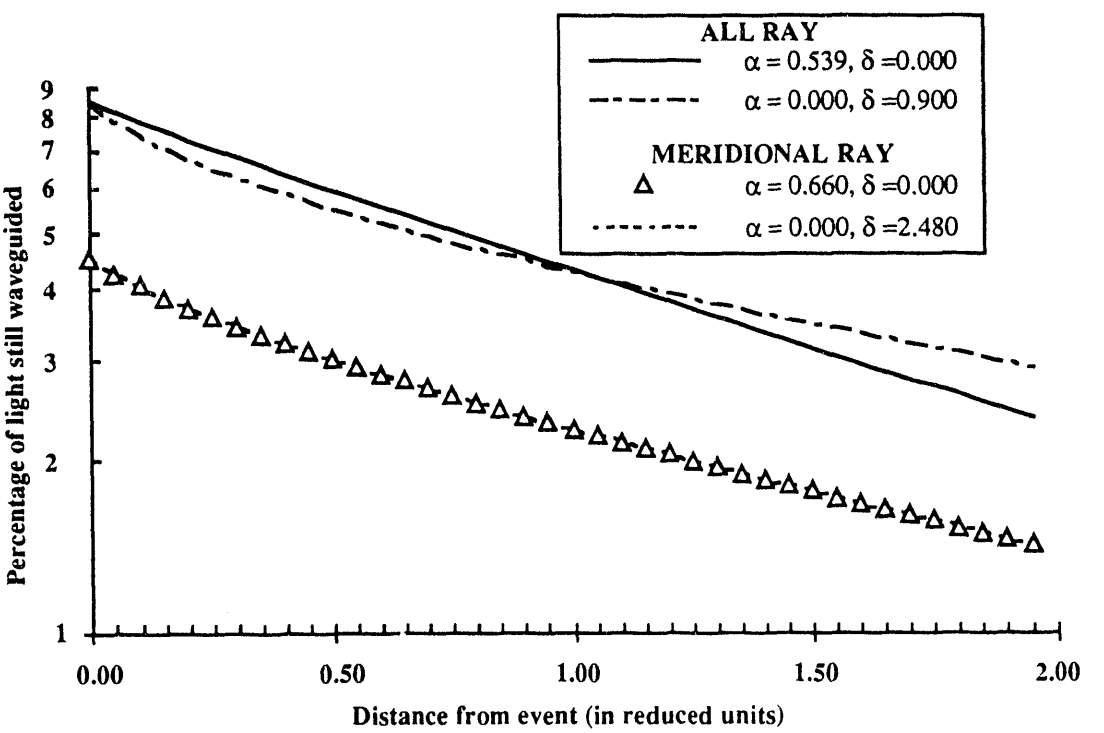

Figure 5. Fraction of total emitted light remaining vs. reduced distance for extremal values of α and δ for all-ray calculations and for meridional ray calculations. Here δ = Δ/2a is the loss-on-reflection coefficient.

Several additional features are evident. First, the total percentage of light captured by the cylinder is about 8.6% compared to the estimate of about 4.5%, which is calculated when only the meridional rays are considered. This difference arises because off-axis emission increases the effective numerical aperture (that is, the angles with respect to the axis of symmetry, θ, for which total internal reflection can occur). This is easy to see. In the condition for total internal reflection,

$$\sin(\theta) \leq [\sqrt{1-(n_2/n_1)^2}]/\cos(\gamma)$$

the factor, $\cos(\gamma)$, which is unity for meridional rays, is less than unity for skew rays. As γ increases, the range of θ for which total internal reflection can occur can increase to include all θ. Second, the intensity drops off far faster than might be expected on the basis of exponential extinction. This occurs because rays with greater θ have greater path length and greater number of interactions with the core/cladding interface in travelling a given axial length of the cylinder.[e] Thus, it is easy to see what is happening. Initially rays at a large range of values of θ are collected. As the point of observation is moved down the axis of the cylinder, the rays with larger angles are found to have suffered greater attenuation than those with smaller angles. The effective capture angle is reduced and the effective numerical aperture is reduced. This phenomenon we refer to as searchlighting.

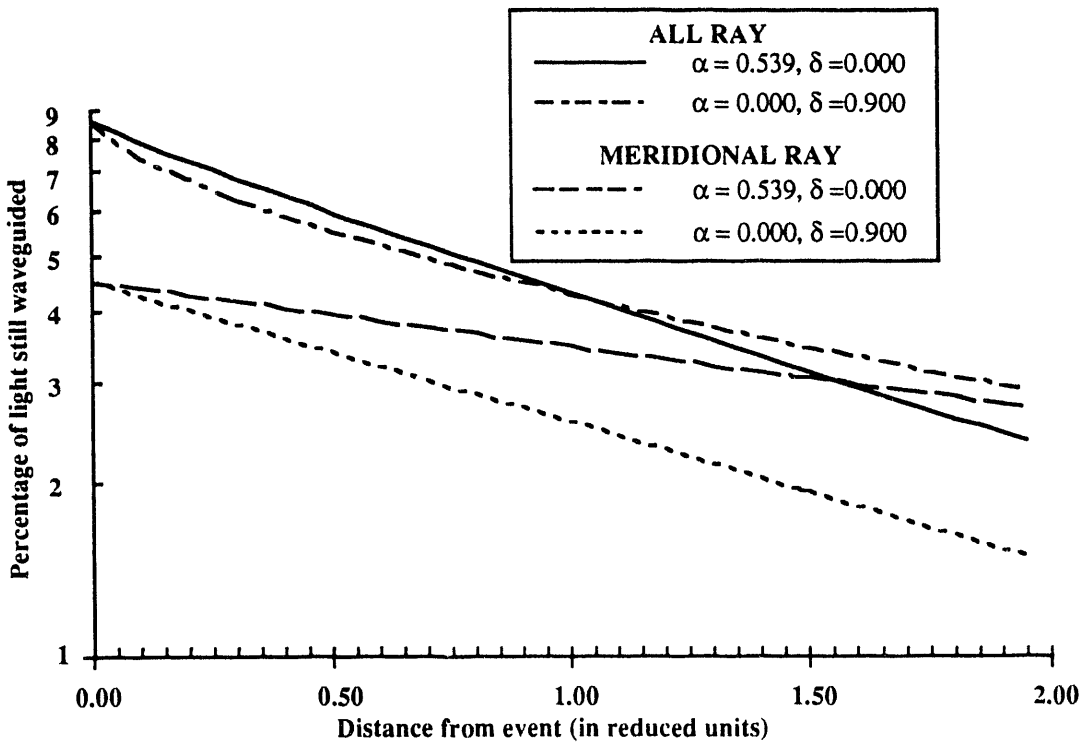

Figure 6. Fraction of total emitted light remaining vs. reduced distance for the same values of α and δ for all-ray calculations and for meridional ray calculations. Here $\delta = \Delta/2a$ is the loss-on-reflection coefficient.

It is worthwhile to compare the results of an all-ray calculation with that for meridional rays alone. Such a calculation was performed in much the same way as for the all-ray calculation. The results for all bulk extinction and all loss-on-reflection are shown

[e] One can think of the extreme case in which $\theta = \pi/2$ for which the ray would bounce around the cylinder, logging considerable distance without creating any progress in the axial direction.

in Figure 5. These calculations show several things. First, there is some non-exponential behavior to the collective loss function. This is not surprising, because there is a mix of rays with different loss per unit distance travelled down the fiber. Second, there is no appreciable difference between the case when the all loss is by bulk extinction and when the loss is all by loss-on-reflection. This occurs for meridional rays because the geometry is simple and the angles of the trapped rays with the axis of the fiber are all small. Third, it is extremely important to note that the scales for the meridional and skew rays in Figure 5 are very different. This is an artifact of the requirement that the fraction remaining be 0.5 at $z = 1$. Figure 6 shows the result of plotting these on the same scale. It is seen that if there is appreciable loss-on-reflection, the region in which the skew rays are important is short and confined to that region near the initial event. On the other hand, if all the loss is by bulk extinction, the attenuation curves are nearly parallel. These results are not surprising. Loss-on-reflection affects skew rays most; bulk attenuation affects all rays nearly equally.

4. Acknowledgements

This work was supported, in part, by the Pacific Northwest Laboratory's Laboratory Directed Research and Development Program. Pacific Northwest Laboratory is operated by Battelle Memorial Institute for the U. S. Department of Energy under contract DE–AC06–76RLO 1830.

5. References

1. W. P. Siegmund, et al., in *Neutrons, X Rays, and Gamma Rays: Imaging Detectors, Material Characterization Techniques, and Applications*, ed. J. M. Carpenter et al., (SPIE Proceedings, Volume 1737, 21-22 July 1992).

2. R. Drougard and R. J. Potter, in *Advanced Optical Techniques*, ed. A. C. S. Van Heel (John Wiley, New York, 1967).

DATE
FILMED
5/20/94
END